# Position/Force Control of an Underwater Mobile Manipulator

**Lionel LAPIERRE, Philippe FRAISSE, Pierre DAUCHEZ**
LIRMM (UMR 5506 CNRS - UM2)
Université Montpellier II
161, rue Ada
34392 Montpellier Cedex 5
{lapierre, fraisse, dauchez}@lirmm.fr

**Abstract**

This paper proposes a new control method applied to an underwater vehicle equipped with a robot manipulator. This control method is based on force control to stabilise the platform when the manipulator works in free or constrained space. The torque produced by the arm on the platform is estimated with a force sensor installed between the base of the manipulator and the vehicle. This allows correcting the position errors of the platform using an external force control loop. This paper presents this control law and shows some simulation results.

## 1 INTRODUCTION

Since few years, the activity in the underwater environment is diversifying. Remotely Operated underwater Vehicle (ROVs) and Autonomous Underwater Vehicles (AUVs) have an important role to play in a number of shallow and deep-water missions for marine science, oil and gas, survey, exploration, exploitation, and military applications. That requires developing new principles and computational techniques to construct and control autonomous or semi-autonomous underwater mobile manipulators, efficient and cost-effective. Many academic or commercial organisations are investigating in different research axis dedicated to communication methods, sonar interpretation, sensor integration techniques, artificial intelligence method for planning, obstacle avoidance, vehicle energy sources and propulsion mechanism, and manipulator-vehicle control scheme. This domain of research

| | Terrest. | Spatial | Sub-sea |
|---|---|---|---|
| Inertial Cor. effects | active | active | active |
| Gravity effects | active | null | neglected (Buoyancy) |
| Viscous effects | neglected | null | active |
| Arm flexibility | neglected | active | neglected |

Table 1: The origins of the reaction torque of the arm on the vehicle

concerns the general problem of mobile manipulation, but the particularities of the underwater environment imposes to imagine new specific methods able to take into account the hydrodynamic phenomena which acts on all the elements of the robot. This specific condition implies an important modification of the dynamic of the immersed global system, and especially concerning the dynamic coupling between the manipulator and the vehicle. There are many ways to take into account the effects of this dynamic coupling, and interesting solutions have been proposed in the different domains of evolution. Every environment (terrestrial, spatial, sub-sea) has its own specifications. This involves that, in front of the same question, there are different solutions to solve the problem of regulation of the dynamic coupling between the arm and the vehicle. We define the physical origins of the action of the arm on the platform according to the application domain (Cf. table 1).

## 1.1 Terrestrial

Most solutions to control the reaction torque of the arm on the platform consist in keeping the robot in stable configuration which permits to neglect the effects of this torque. These methods use the redundancy of the system to find trajectories which guaranty the stability of the vehicle and the optimal manipulability ([20], [21], [18], [17]). S. Dubowsky [3] proposes to compensate dynamically the reaction torque of the arm on the vehicle using moving counterweights to insure that the ground projection of the centre of mass of the global system is in the sustentation polygon of the vehicle. We remark that all these methods use the gravity action to stabilise the system.

| | Effect | Origin |
|---|---|---|
| Added mass | Modification of the dynamic | Kinetic Energy of surrounded fluid |
| Drag forces | Modification of the dynamic | Viscosity of the fluid |
| Buoyancy | No more gravity effect | Density of the fluid |
| Currents | Current loads | Fluid |
| Waves | Forced oscillations | acceleration |

Table 2: Hydrodynamic phenomena

## 1.2 Spatial

The main difference between spatial and terrestrial environment is that in space, there is no domain reaction. Excepted the solar pressure, there is no external perturbations. So, it is possible to apply theoretical models without restrictive hypothesis. With a precise identification of the internal parameters of the system, it's possible to apply classic control laws [12]. A good model of the system allows estimating with a good precision the value of the reaction torque of the arm on the platform. Then, with this information we can apply classic control laws with internal force control loop to correct on-line the perturbations coming from the arm [15].

## 1.3 Sub-sea

Sub-sea Some specific phenomena characterise the sub-sea environment. We can analyse the consequences of these phenomena on the comportment of the robot (Cf. table 2).

Unlike the spatial domain, modelling the sub-sea environment is very complex. The main problem encountered is the precise estimation of the hydrodynamic coefficients. Furthermore, the coefficients vary according to the temperature, depth, salinity, winds... We distinguish four methods to solve this problem. J. Yuh ([22], [23]) proposes an algorithm which permits the identification of these parameters on-line, analysing the behaviour of the robot. This method costs a long computation time. An efficient estimation of the position can avoid these constraints [13]. But it is very difficult to guarantee good position estimation without a structured environment. The station keeping permits to anaesthetise the vehicle to the arm reaction. It

needs a supplementary mechanical structure to clamp the robot. N. Kato [KAT 96] proposes an original method to use these arms like paddles outwards the clamped situation to counter the disturbing action of the moving arm. In conclusion of his works related to the European project UNION, J. Kiener [10] underlines the necessity to control dynamically the torque produced by the arm on the vehicle.

The main difficulty in the regulation of arm effects on the platform is to estimate precisely the torque produced by the arm on the platform. We have chosen to measure it with a force sensor installed on the link between the arm and the vehicle. This measurement is used in an internal force control loop to correct the command of the vehicle thrusters.

This paper is organised as follow. The section II is concerned with the underwater environment action modelling on a moving immersed body, without considering current loads. The consideration and evaluation of the hydrodynamic forces acting on a rotational moving object, like the elements of the manipulator, is presented. Section III presents the dynamic modelling of the combined model vehicle-manipulator. The force sensor, on the link between the arm and the vehicle, is modelled with the Newton-Euler approach. Section IV presents some simulation results which presents the effects of hydrodynamic phenomena on the robot behaviour, and their implications on the dynamic coupling between the arm and the vehicle. These results are compared to other simulations and experimental results presented in [DUN 98] and [LAI 96], validating our model. Section V introduces a control law design for reduction of the dynamic coupling when the arm moves in free space. This control law is modified and applied to the case of a task in a constrained space in the section VI. Some considerations about stability analysis are presented. Section VII is concerned with technical considerations and presents a new method to control naturally the dynamic coupling. Section VIII provides conclusions on the advantage and disadvantage of this technique.

# 2 Environment action modelling

The three-dimensional equations of motion for hydrodynamically shaped underwater vehicle are generally developed using a body fixed coordinate frame, $(X_P, Y_P, Z_P)$, and a global coordinate frame $(X_0, Y_0, Z_0)$. The body coordinate frame has components of motion given by the six velocity components $[u(t), v(t), w(t), p(t), q(t), r(t)]$, relative to a constant velocity coordinate frame moving with the ocean current, uc, and, according to the SNAME nomenclature [19] described in figure 1, the velocity vector is represented as

:

$$v_1 = \begin{pmatrix} u : \textbf{longitudinal vel.} \\ v : \textbf{transverse vel.} \\ w : \textbf{normal vel.} \end{pmatrix}, \qquad v_2 = \begin{pmatrix} p = \dot{\phi} : \textbf{roll vel.} \\ q = \dot{\theta} : \textbf{pitch vel.} \\ r = \dot{\psi} : \textbf{yaw vel.} \end{pmatrix} \tag{1}$$

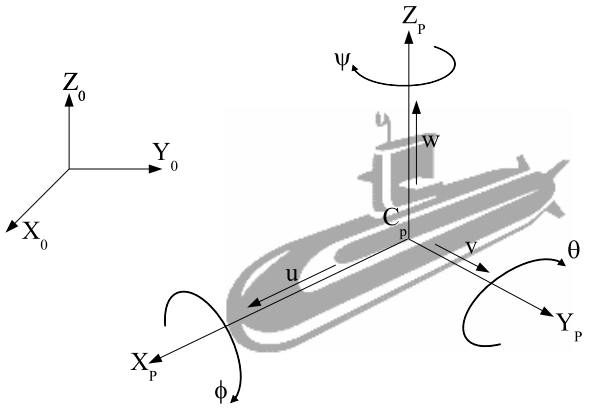


Figure 1: situation description of an immersed body

In our study case, we have chosen to develop a two dimensional model. The situation vector $\eta$ and the velocity vector $v$ , of the vehicle are given in equations (2).

$$\begin{array}{ll} \eta_1 = (x, y)^T & v_1 = (u, w)^T \\ \eta_2 = \theta & v_2 = \dot{\theta} \\ \eta_3 = (x, z, \theta)^T & v_3 = (u, v, \dot{\theta})^T \end{array} \tag{2}$$

The general considered significant hydrodynamic phenomena are: added mass, drag forces, buoyancy, waves and current effects. We neglect wave's effects and consider the current load as null.

## 2.1 Added Mass

Generate a movement of an immersed body implies to provide the necessary energy to accelerate the mass of the body and the mass of the surrounded fluid particles, which accompany the movement. This adding kinetic energy is function of the body shape and modifies the dynamic behaviour of the immersed system, which apparently reacts like heavier, according to its front shape. This phenomenon has been described in general terms by Fossen [7]

as follow (with the both hypothesis of a three orthogonal symmetrical body and independent added mass forces and torques for low velocities):

$$\begin{pmatrix} F_A^T \\ F_A^T \end{pmatrix} = -M_A\dot{v} - C_a(v)v \tag{3}$$

The computation method of the MA and CA coefficients is given in [7], [14] and [8].

## 2.2 Drag Forces

This phenomenon is caused by the viscosity of the fluid. The general form of the drag force is

$$D_f = -\frac{1}{2}\rho C_D A|v|v \tag{4}$$

with $\rho$ the fluid density, $A$ the frontal area, $C_D$ the drag coefficient and $v$ the relative velocity of the body compare to the fluid. The drag coefficient $C_D$ is estimated in function of the Reynold's number of the body, which defines the type the fluid flow around the body. A modelling restrictive hypothesis imposes a limitation of the Reynold's number to guaranty a laminar flow all around the body surface. This limitation implies a velocity limitation for the body, $v_{max}$. The details of computation of the Reynold's number is given in [14] and [5] for elementary body shapes. A specific integrative calculation is necessary concerning objects moving in a circular way, like the elements of the manipulator, that we consider as cylinders. It is also assumed that the cylinders are fully submerged and the effects of nearby objects and solid boundaries are neglected.

We consider an element $dx$ of a link of the manipulator, situated at $x$ from the join. This element has an absolute linear velocity $V_{M1}(x)$. $V_n(x)$ is the normal component of $V_{M1}(x)$. The drag force and moment engendered by this element are:

$$\begin{array}{l} dF_D(x)|_{R1} = -\frac{1}{2}\rho C_D|V^n(x)|V^n(x)2rdx \\ dM_D(x)|_{R1} = -\frac{1}{2}\rho C_D|V^n(x)|V^n(x)2rxdx \end{array} \tag{5}$$

We determine the drag force and moment of the link with an integrative computation along the length of the link.

$$\begin{array}{l} F_{Di} = -\frac{1}{2}\rho C_D 2r \int_0^{li} |V^n(x)|V^n(x)dx \\ M_{Di} = -\frac{1}{2}\rho C_D 2r \int_0^{li} |V^n(x)|V^n(x)xdx \end{array} \tag{6}$$

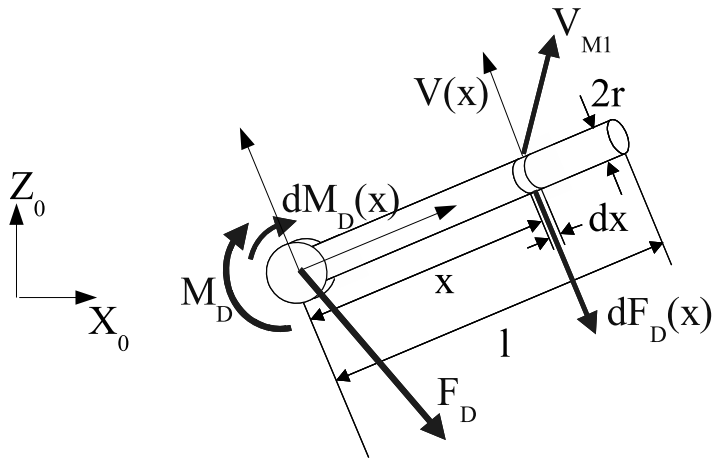


Figure 2: Drag force integrative computation

## 2.3 Buoyancy and Gravity

The classic form of the buoyant force is:

$$\overrightarrow{B} = -\rho V_{fl}\,\overrightarrow{g} \tag{7}$$

with $V_{fl}$, the body volume and $g$ the gravitational acceleration. The gravity has to be considered in the fluid, and takes the classic form:

$$\overrightarrow{W} = m\,\overrightarrow{g} \tag{8}$$

with $m$, the body mass. Rigorously, the $g$ value varies with the depth. Nevertheless, we consider it as constant in all the simulations. Notice that the static equilibrium is dependant of the condition:

$$G(\eta) = \begin{pmatrix} (m-\rho V)g\sin\theta \\ -(m-\rho V)g\cos\theta\sin\phi \\ -(m-\rho V)g\cos\theta\cos\phi \\ (mY_G-\rho VY_F)g\cos\theta\cos\phi - (mZ_G-\rho VZ_F)g\cos\theta\sin\phi \\ -(mZ_G-\rho VZ_F)g\sin\phi - (mX_G-\rho VX_F)g\cos\theta\sin\phi \\ (mX_G-\rho VX_F)g\cos\theta\sin\phi + (mY_G-\rho VY_F)g\sin\phi \end{pmatrix} \tag{9}$$

with $C_G = (X_G, Y_G, Z_G)^T$ the centre of mass of the body and $C_F = (X_F, Y_F, Z_F)$ the centre of mass of the displaced fluid. In another way, the static equilibrium depends of the position of the geometric centre and the centre of mass of the body.

## 2.4 GLobal Environment Action Model

The environment action on an immersed body is expressed as follow :

$$\begin{pmatrix} F \\ M \end{pmatrix}_{Env} = -M_A\dot{v} - C_a(v)v + D_f(v) + G(\eta) \tag{10}$$

# 3 Global Vehicle-Manipulator combined dynamic model

We have chosen a spherical platform with a two cylindrical links manipulator. The evolution space is limited at two dimensions (figure 3).

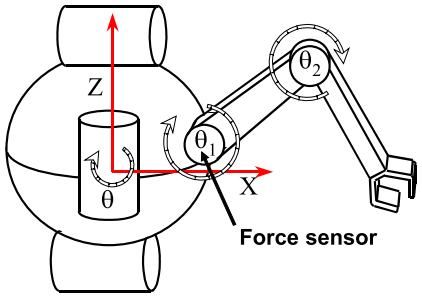


Figure 3: The underwater vehicle

We define four coordinates frames : $R_0 : (O, X_0, Y_0, Z_0)$ the absolute frame ; $R_P : (C_P, X_P, Y_P, Z_P)$ the platform attached frame ; $R_1 : (C_1, X_1, Y_1, Z_1)$ and $R_2 : (C_2, X_2, Y_2, Z_2)$ the two manipulator links attached frames. The position of the vehicle is described with the 3 coordinates vector $P = (x_P z_P \theta_P)^T$, and for the two links manipulator $q_b = (\theta_1\ \theta_2)^T$, and the global coordinates system $q = (\eta_P q_b)^T$ (cf. figure 4).

The transformations between the different frames are define as described in the figure 5.

The geometric characteristics of the robot and the environment are chosen as described in the table 3.

The combined dynamic model is developed with the Lagrange-Euler formalism based on energy considerations. We obtain the equation 11.

$$\Gamma_{ext} = A(q)\ddot{q} + H(q, \dot{q}) + G(q) \tag{11}$$

with $A$ the system inertial matrix (with added mass), $H$ the Coriolis and centrifugal vector (with added mass), $G$ the hydrostatic equilibrium vector and $\Gamma_{ext}$ the external forces vector. The external forces applied to the robot

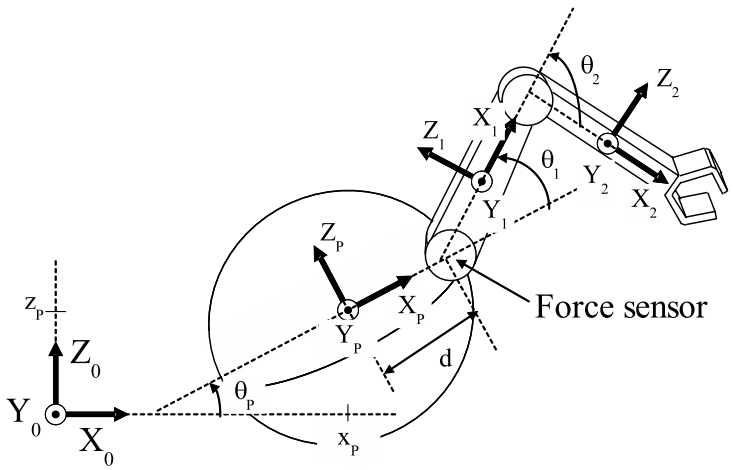


Figure 4: Frames Definition

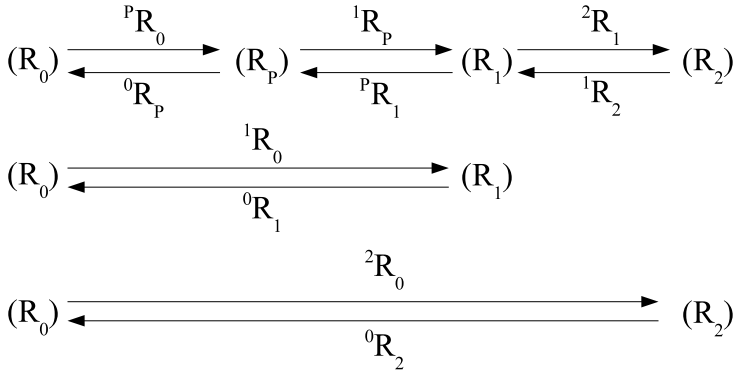


Figure 5: Frames Transformation Definition

| Vehicle | Arm $1^{st}$ link | Arm $2^{nd}$ link |
|---|---|---|
| Robot Geometric characteristics | | |
| Radius: 0.5m | Lengh:1m | Lengh:1m |
| $d = 0.25m$ | Radius:0.05m | Radius:0.05m |
| Mass:523.6kg | Mass:8.04kg | Mass:8.04kg |
| Added Mass | | |
| $m^x_{a.p}$=261.8kg | $m^x_{a.2}$=0.134kg | $m^x_{a.2}$=0.134kg |
| $m^y_{a.p}$=261.8kg | $m^y_{a.2}$=2.41kg | $m^y_{a.2}$=2.41kg |
| $I_{a.p}$=0kg.m$^2$ | $I_{a.2}$=0.025kg | $I_{a.2}$=0.025kg |
| $M_{a.p} = \begin{bmatrix} m^x_{a.p} & 0 & 0 \\ 0 & m^y_{a.p} & 0 \\ 0 & 0 & I_{a.p} \end{bmatrix}$ | $M_{a.1} = \begin{bmatrix} m^x_{a.1} & 0 & 0 \\ 0 & m^y_{a.1} & 0 \\ 0 & 0 & I_{a.1} \end{bmatrix}$ | $M_{a.2} = \begin{bmatrix} m^x_{a.2} & 0 & 0 \\ 0 & m^y_{a.2} & 0 \\ 0 & 0 & I_{a.2} \end{bmatrix}$ |
| Drag Coefficients | | |
| $C_{Dp}$=0.4 | $C_{D1}$=1 | $C_{D2}$=1 |
| Environment characteristics | | |
| Grav. Acc. $g = 10m.s^-2$ | Water Density $\rho = 1025kgm^{-3}$ | Water Viscosity $v = 1.56.10^{-6}m^2s^{-1}$ |

Table 3: System Characteristics

include the drag forces and the actuators action. The global dynamic model is written as:

$$F_{act} = A(q)\ddot{q} + H(q, \dot{q}) + D(\dot{q})\dot{q} + G(q) \tag{12}$$

with $D$, the drag forces vector and $F_{act}$, the actuators action vector.

## 3.1 Actuators modelling

We consider the model for the arm actuators as developed in [1] for a PUMA 560. The platform thrusters are included considering a linear model.

$$\begin{aligned} \Gamma_b &= f(U_b) \\ F_p &= K_p U_p \\ F_{act} &= (F_p\, \Gamma_b)^T \end{aligned} \tag{13}$$

with $\Gamma_b$ the torques exerted by the manipulator actuators, $F_p$ the platform action thrusters, $K_p$ the static amplification of the platform thrusters and $U_b$ and $U_p$ the actuators control voltage. $F_{act}$ is a 5 dimensions vector.

## 3.2 Force sensor modelling

The Lagrange-Euler formalism cannot provide the structure internal forces (only along the joint axis). Nevertheless, the Newton-Euler formalism equations of motion are a set of forward and backward recursive equations, with the dynamics and kinematics of each link referenced to its own coordinate system, which by this way, checks all the forces and torques on each link and provides the efforts present on the link between the arm and the vehicle, where we virtually install the force sensor. The manipulator-vehicle dynamic interaction measurement takes the following form :

$$F_{Capt.Eff} = (F_x \; F_z \; \Gamma_{b1})^T \tag{14}$$

with $F_x$ and $F_z$ the linear forces on the rotational link between the arm and the vehicle, and $\Gamma_{b1}$ the torque presents on this link. $F_{Capt.Eff}$ is a 3 dimensions vector.

## 3.3 Velocity limitation

The model chosen for the drag phenomenon imposes a velocity limitation which guaranties that the flow around the immersed objects stays in a laminar regime. This limitation is function of the Reynold's number of each solids composing the robot, which are dependant of their geometry. By hypothesis, our robot is composed by spherical and cylindrical objects. The maximum absolute velocity for the spherical platform is $U_{max.Sph} = 0.46m.s^{-1}$, and all the points of the manipulator have to move with a velocity less than $U_{max.Cyl} = 4.68m.s^{-1}$. To be exploitable, this limitation have to be converted to articular velocity limitation. Under the both pessimistic hypothesis that $U_{max.Sph} = 0.3m.s^{-1}$ and that the articular velocity limitations is the same for all the manipulator links, and using the kinematics relations between the platform the manipulator links and the end effector, we establish the following relation which describe the maximum articular velocities for five links of the robot.

$$\dot{q}_{max} = [0.3m.s^{-1} \; 0.3m.s^{-1} \; 1rad.s^{-1} \; 1rad.s^{-1} \; 1rad.s^{-1}]^T \tag{15}$$

Respecting this condition, we guaranty that all the points of the robot stay in the domain of laminar flow, and the validity of the model employed.

# 4 Validation of the model. Manipulator-vehicle dynamic interactions

We verify in this section that our simulator responses are coherent with the attempted behaviour.

## 4.1 Drag effects

The effects of the drag phenomenon are showed on the simulator with the test described in figure 6 . The arm is deployed in the initial position. It is then enslaved to follow a polynomial trajectory with a classic PD control law. During this test, the plat-form is free and fully undergoes the effects of dynamic interactions.

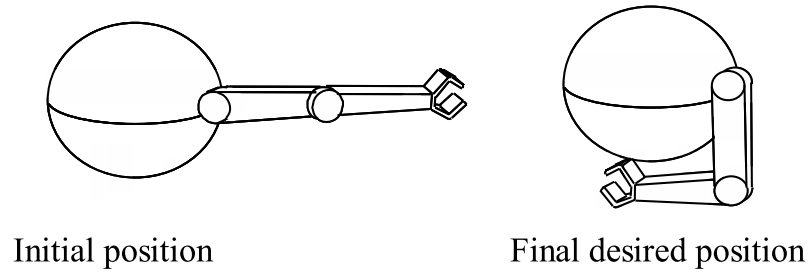


Figure 6: Drag effects test

This simulation results are presented in the 3, where we notice that the drag phenomenon induces an increased effect of the dynamic coupling, and engender a damping effect, opposed to the velocity, on every moving robot element.

## 4.2 Added Mass effects

The added mass phenomenon implies a modification of the dynamic of an immersed body. The 7 presents the platform step response. The immersed object like heavier, according to the movement direction, and the frontal shape presented perpendicularly to the velocity.

## 4.3 Comparison with other simulation results

M.W Dunningan and G.T. Russel [4] have developed a simulator based on the ANGUS vehicle model. This vehicle is composed by a cubic platform with

| Evolution of the platform position | Evolution of the dynamic interation |
|---|---|
| *Without drag: dotted gray line, with drag: black line* | |

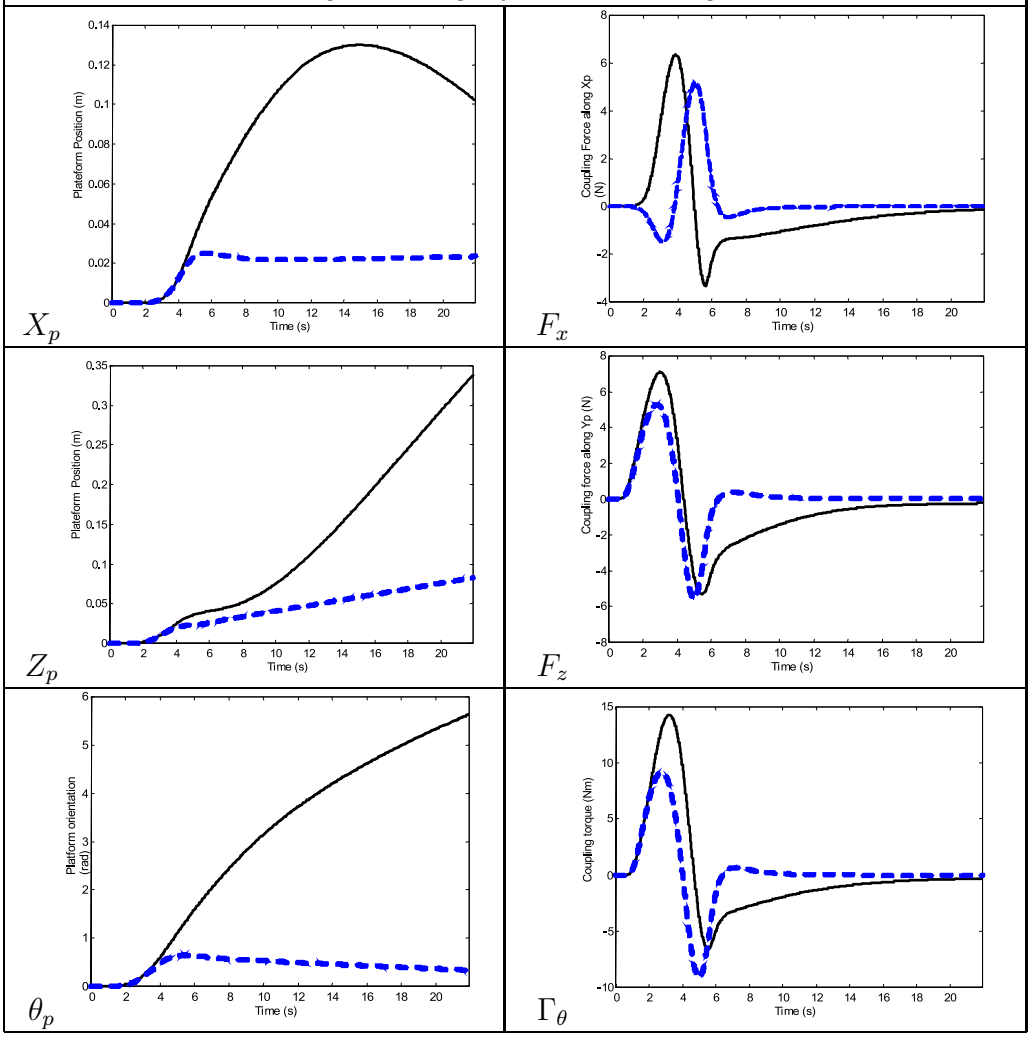


Table 4: Drag effects

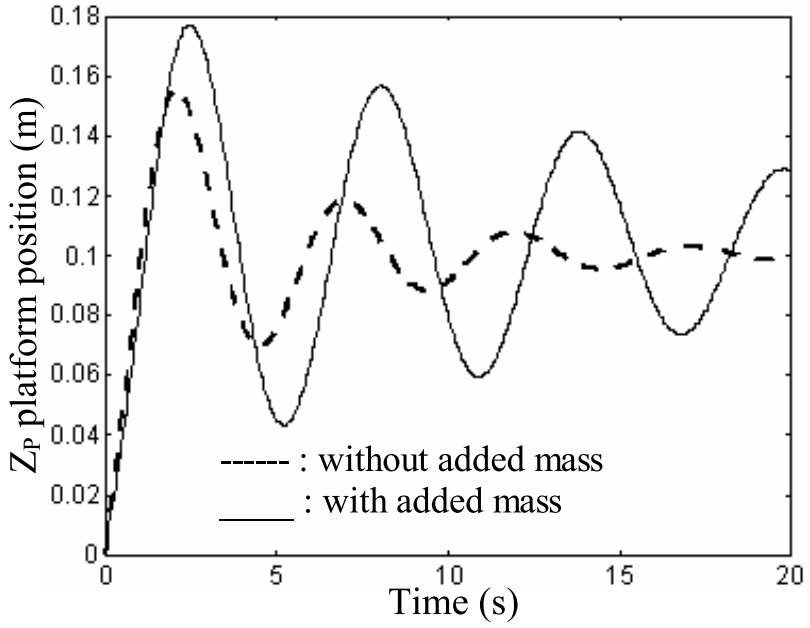


Figure 7: Added mass effects (platform step response)

a three degrees of freedom manipulator. The first link of the manipulator is enslaved to follow the trajectory described in following equations.

$$\begin{gathered}
\theta_D(t) = \theta_D(0) + \frac{\Delta}{2\pi}(\omega t - \sin(\omega t)),\ 0 \leq t \leq t_f \\
\theta_D(t) = \theta_D(t_f),\ t > t_f \\
\dot{\theta}_D(t) = \frac{\Delta}{t_f}(1 - \cos(\omega t)),\ 0 \leq t \leq t_f \\
\ddot{\theta}_D(t) = \frac{2\pi\Delta}{t_f^2}\sin(\omega t),\ 0 \leq t \leq t_f \\
\dot{\theta}_D(t) = \ddot{\theta}_D(t) = 0,\ t > t_f \\
\omega = \frac{2\pi}{t_f},\ \Delta = \theta_D(t_f) - \theta_d(0)
\end{gathered} \tag{16}$$

Three simulations are computed with the following characteristic : $-\pi/4 \leq \theta_1 \leq \pi/4$, $\theta_2 = \theta_3 = 0$, $t_f = 1, 2, 5s$. Dunnigan and Russel obtain the results of the figure a in the table 5, concerning the evolution of the yaw angle. Because of our different frame definition, we program the same test on our simulator, and compare the evolution of the pitch angle to Dunnigan and Russel results (table 5).

## 4.4 Comparison with experimental results

This comparison is necessary to verify the coherence of our simulation results. T.W McLain, S. M. Rock and M. J. Lee [11] have made experiments

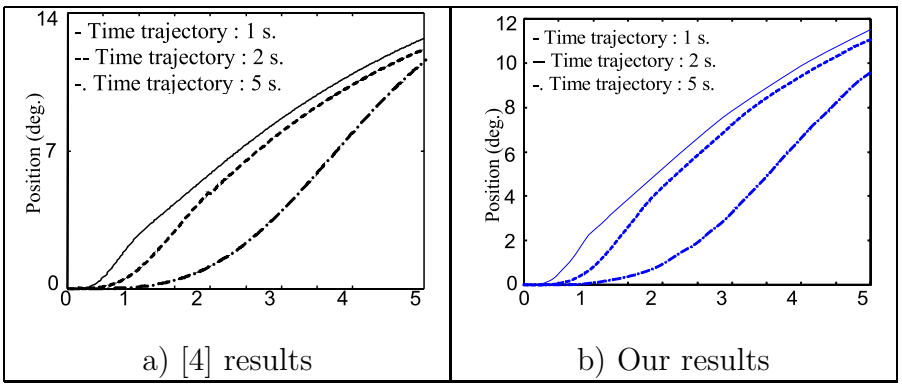


Table 5: Comparison with Dunningan results

on the OTTER submarine vehicle with a one degree of freedom manipulator mounted on it. They carry out a test consisting in a sinusoidal trajectory generation for the arm, measuring the evolution of the reaction torque between the manipulator and the platform. They obtain the results of the figure 10a. Blocking the second link of the manipulator, the same test on our simulator brings the results of the figure b of the table 6.

We now consider our simulator as valid.

# 5 Control law design for reduction of the dynamic coupling in free space

## 5.1 Effects of the dynamic coupling. Open loop control

A preliminary test of the vehicle is presented when a PID control law controls the arm (figure 8). The thrusters of the platform are not considered in this test.

The desired position of the system is $P = [000\pi/2\pi/2]^T$ . The simulation results are presented figures 9 and 10. Final arm positions are reached in 15s.

The orientation of the platform tends to 5 radians. That is a very important disturbance.

## 5.2 Position control

The first way to compensate the action of the arm on the platform is to control the position of vehicle thanks to its absolute position sensors. Considering perfect sensors, we present in figure 12 the simulation result of the

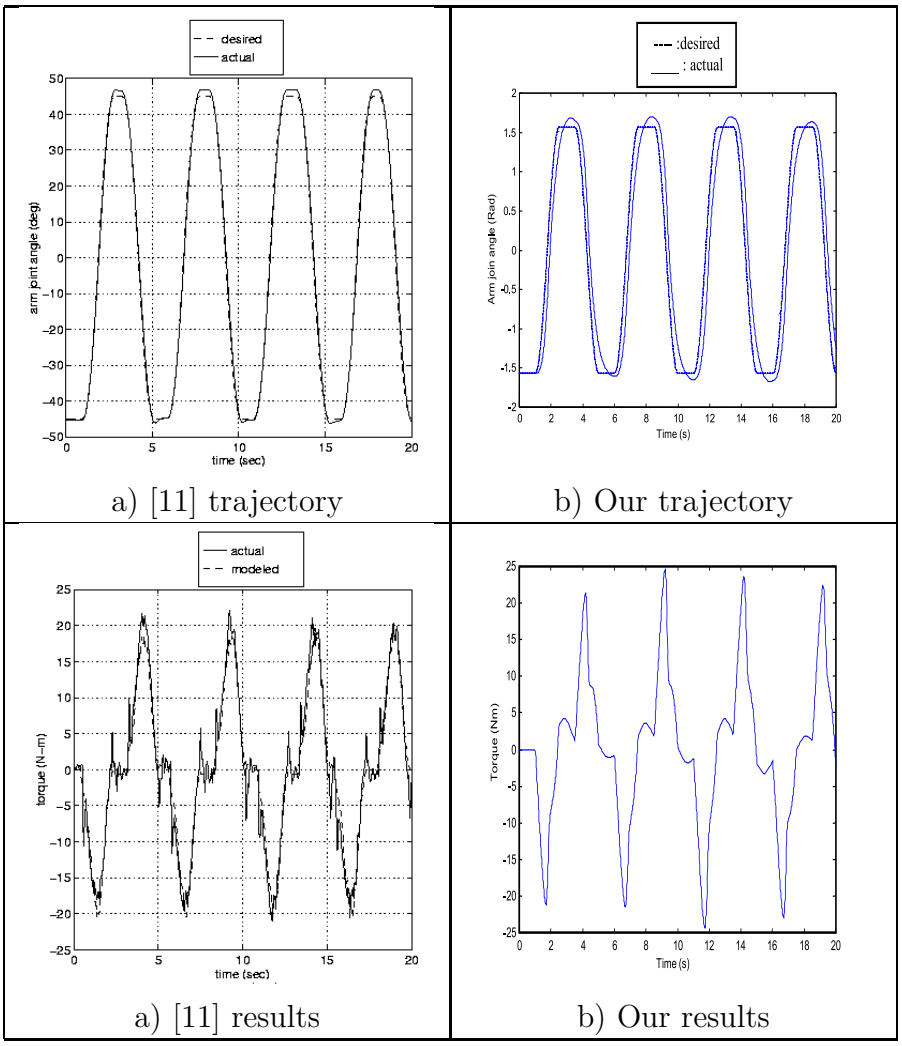


a) [11] trajectory | b) Our trajectory

a) [11] results | b) Our results

Table 6: Comparison with McLain results

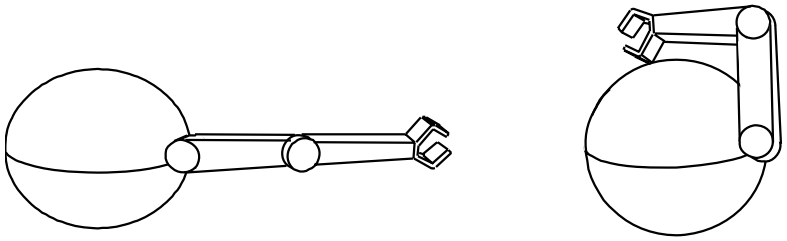

Initial position | Desired position

Figure 8: Open loop test

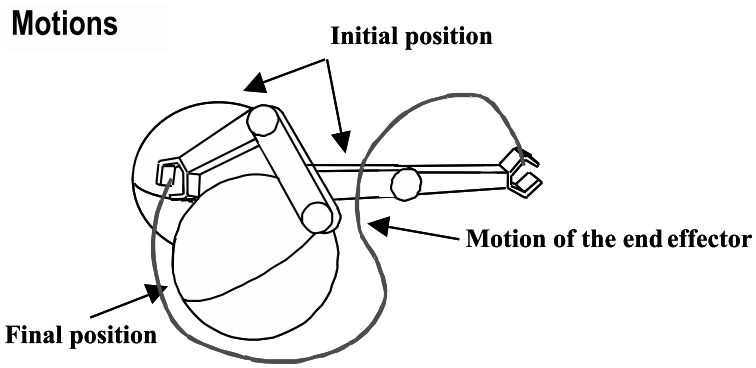


Figure 9: End effector trajectory

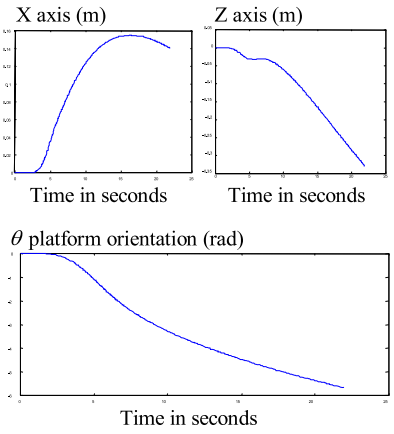


Figure 10: Open loop result, motion of the platform

test described in figure 11, with the platform position control loop schematized in figure 11.

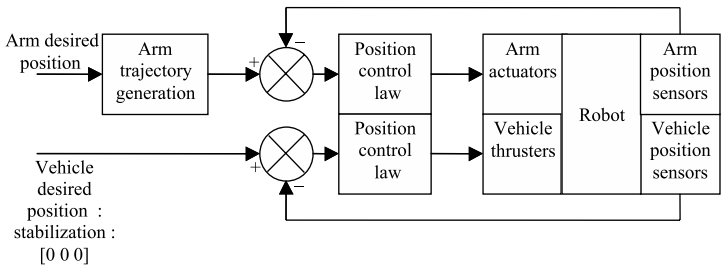


Figure 11: Position control scheme

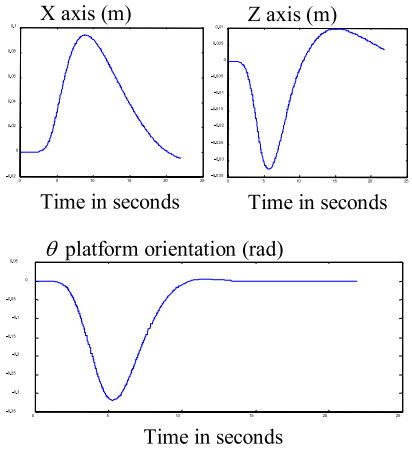


Figure 12: position control, results

The main problem is the low precision and bandwidth of this sensors used to undersea conditions. A robust position control law is not enough to stabilize the platform when the arm moves. In order to improve the solution of this problem we add an external force control law on the position loop to minimize the interaction forces between the platform and the arm.

## 5.3 Compensation in free space

The compensation of the disturbance when the arm moves in the free space is obtained by an external force control loop (figure 13). The force values are measured with the force sensor installed on the link between the arm and the vehicle, as modeled in section III. The goal of this compensation is to

eliminate the interaction force between the manipulator and the platform. This measurement uses an external force control loop to correct the command of the vehicle thrusters.

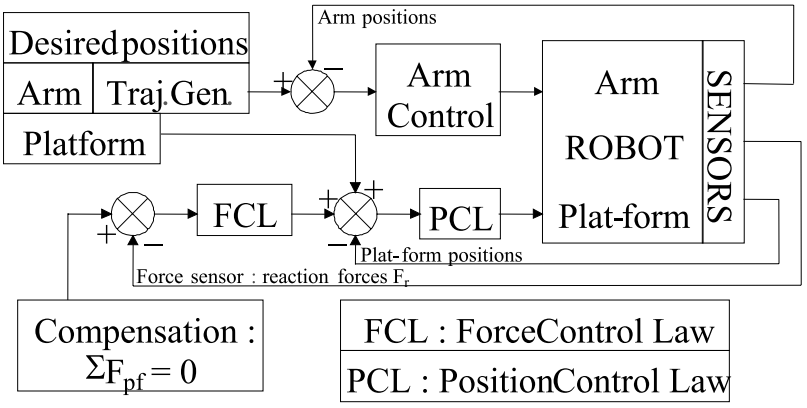


Figure 13: external force control law

The force vector read on the sensor is defined as $F_{Capt.Eff} = [F_{rx}\, F_{rz}\, \tau_r]^T$. Including the torques present on the links of the arm, which can be easily known using torque sensors, we generalise the force vector as 5 dimensional vector $F_{Capt.Eff} = [F_{rx}\, F_{rz}\, \tau_r\, \tau_1\, \tau_2]^T$. Which, in the case of the compensation in free space, becomes $F_{Capt.Eff} = [F_{rx}\, F_{rz}\, \tau_r\, 0\, 0]^T$. The desired position of the platform is computed such that

$$P_d^* = P_d + \Delta P_d \tag{17}$$

where

$$\Delta P_d = K_p \tilde{F} + K_i \sum_{n=0}^{\infty} \tilde{F}_n T_e \tag{18}$$

With $\tilde{F} = F_d - F_r$ , the force error vector, $K_p$ and $K_i$ are diagonal matrices 5x5 respectively proportional and integral gain matrix and $T_e$ is the sampling period. The desired force vector $F_d = [00000]^T$. The control vector $F_c$ can be written as:

$$F_c = K_p \tilde{P}_n + \frac{K_d}{T_e}(\tilde{P}_n - \tilde{P}_{n-1}) + K_i \sum_{n=0}^{\infty} \tilde{F}_n T_e \tag{19}$$

With $\tilde{P} = P_d^* - P$ . The desired force vector has to be equal to zero to eliminate the interaction force between the manipulator and the platform.

In figure 14, we obtain some interesting results, using external force control loop. This force control loop reduces the disturbances effetcs.

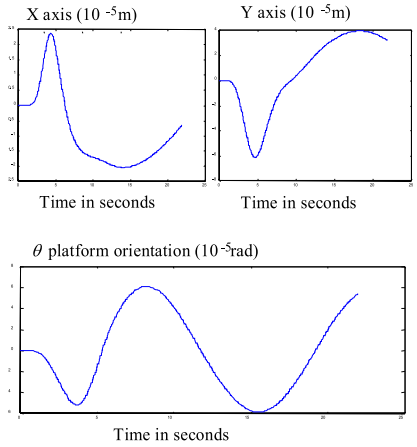


Figure 14: External Force control law, results

The position errors of the vehicle are globally divided by 1000. The external force control loop is a great improvement for underwater mobile manipulator.

# 6 Control law in constrained space

The previous solution allows to compensate the disturbances caused by the movement of the arm. This solution can be used to control the force exerted by the manipulator on the environment.

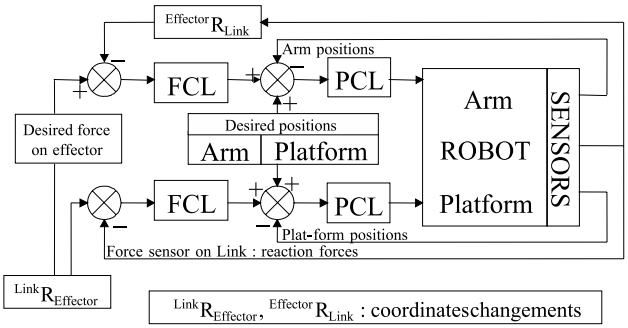


Figure 15: generalized external force control law

The external force loop is used to control in force a manipulator. We propose to modify the previous control equation (19) in order to obtain the

compensation and the force control loop for the vehicle (figure 15) to obtain a satisfying response of the robot during the task described in figure 16.

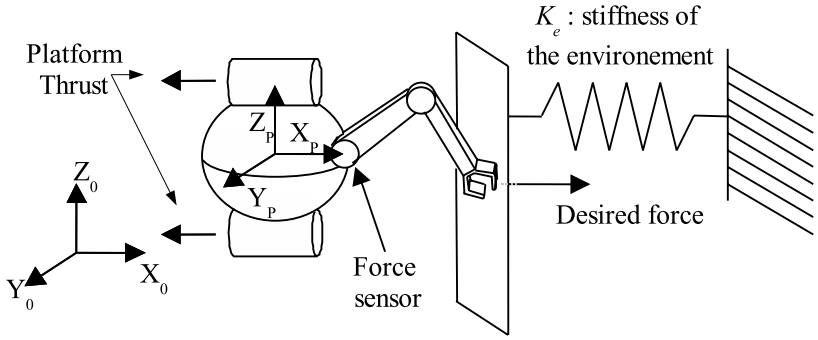


Figure 16: Mobile manipulator in constrained space

A mono-dimensional model arm-vehicle when the manipulator pushes on the environment is given in figure 17.

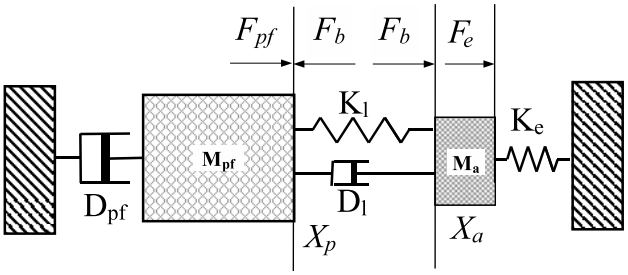


Figure 17: Contact model

The equations are given in (20).

$$\begin{aligned} F_a - K_e X_a - K_l \tilde{X}_{ap} - D_l \dot{\tilde{X}}_{ap} - M_b \ddot{X}_a = 0 \\ F_{pf} - F_a - D_{pf} X_{pf} + K_l \tilde{X}_{ap} + D_l \dot{\tilde{X}}_{ap} - M_{pf} \ddot{X}_{pf} = 0 \end{aligned} \tag{20}$$

where $F_a$ is a force due to the actuators of the arm, $K_e$ is the stiffness of the environment, $K_l$ is the stiffness of the link between the arm and the platform (force sensor), $D_l$ the damping friction, $M_a$ the mass of the arm, $M_{pf}$ the mass of the platform, $F_{pf}$ the force of the platform due to the thrusters and $\tilde{X}_{ap} = X_a - X_p$ . The equations (20) allows us to determine the following asymptotic condition:

$$F_a|_{t\to\infty} = F_{pf}|_{t\to\infty} = F_{xd}|_{t\to\infty} \tag{21}$$

$F_{xd}$ is desired force on the environment along $X$ axis. This result allows us to determine the following equations.

$$\begin{array}{c} F_r = [F_x\ F_z\ \tau_r\ \tau_1\ \tau_2]^T \\ F_d = [F_{xd}\ F_{zd}\ 0\ \tau_{1d}\ \tau_{2d}]^T \\ \begin{bmatrix} \tau_1 \\ \tau_2 \end{bmatrix} = J^t \begin{bmatrix} F_x \\ F_z \end{bmatrix} \end{array} \tag{22}$$

with $J^t$ is the 2x2 Jacobian matrix of the arm.

Using equations (17) and (18) with the vector $\tilde{F}$ we obtain a force control vector such that the equation (19). The main difference between the position (free space) and the force control law is the force error vector $\tilde{F}$ . We have an hybrid position/force control equation for underwater mobile manipulator based on external force control. We can define a generalized vector $F_r$ to control in position and force the mobile manipulator such that :

$$F_r = [F_x\ F_z\ \tau_r\ \alpha\tau_1\ \alpha\tau_2]^T \tag{23}$$

with $\alpha = 1$ in force control, and $\alpha = 0$ in position control to compensate the interacting forces between the arm and the platform. A simulation result is presented figure 18. The mobile manipulator pushes on the environment along $X$ axis.

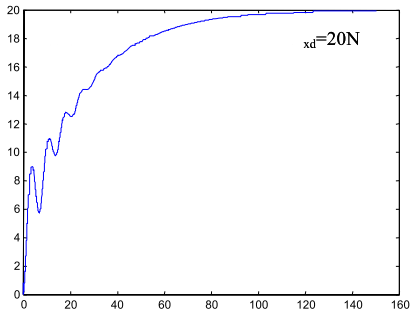


Figure 18: Force control, result

We obtain a satisfying force response of the arm on the environment (figure 18). The arm pushes on the environment and the thrusters of the platform compensate the action of the arm at its base, fixed on the platform. The platform keeps its situation stable during the arm works. This implies for the platform to exert the desired force on the base of the manipulator (equation (21)).

# 7 Position/force control on a trajectory

Some new tests are carried out, considering the robot following a linear trajectory along a curved environment (figure 19). The goal is, for the robot, to follow the trajectory applying a constant effort on the curved environment.

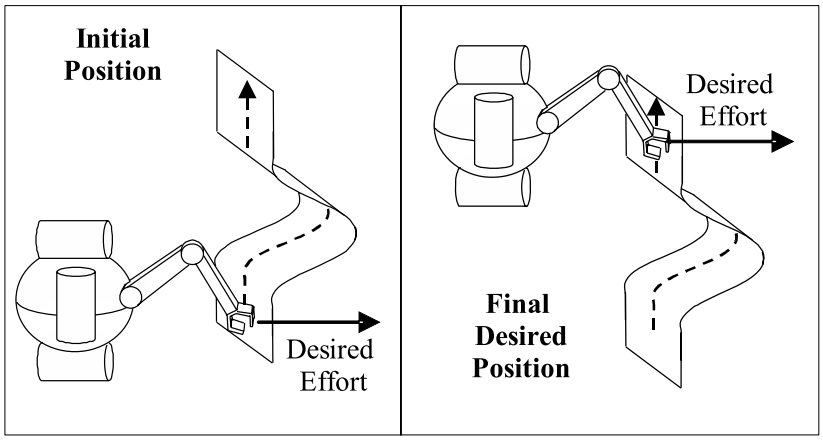


Figure 19: force control on a trajectory

The control law is simply modified to engender on the plat-form a vertical linear movement along the $Z$ axis. The environment presents a sinusoidal variation of $20cm$ amplitude. The desired effort is $40N$. The results are given in the table 7.

The results of the table 7 show a satisfying force response. The platform reacts in a correct way, moving to compensate the modification of the environment. As previous, it reacts slowly, according to its own dynamic. On the other hand, the arm is moving faster and compensate the slow platform reaction. By this way, the desired effort can be applied along the trajectory. The control law coefficients have been adapted to the dynamic of the arm and the platform, according to the results of E. O. DIAZ [2], working on singular perturbations theory. Another criterion useful to compute control coefficients is to notice that the natural arm compliance (links and mechanical compliance, active compliance of the control loop) must be lower than the environment compliance [6].

# 8 Technical consideration

Considering the difficulty to use a force sensor in underwater condition ( marinisation, calibration, cost), we have investigated a method to realize

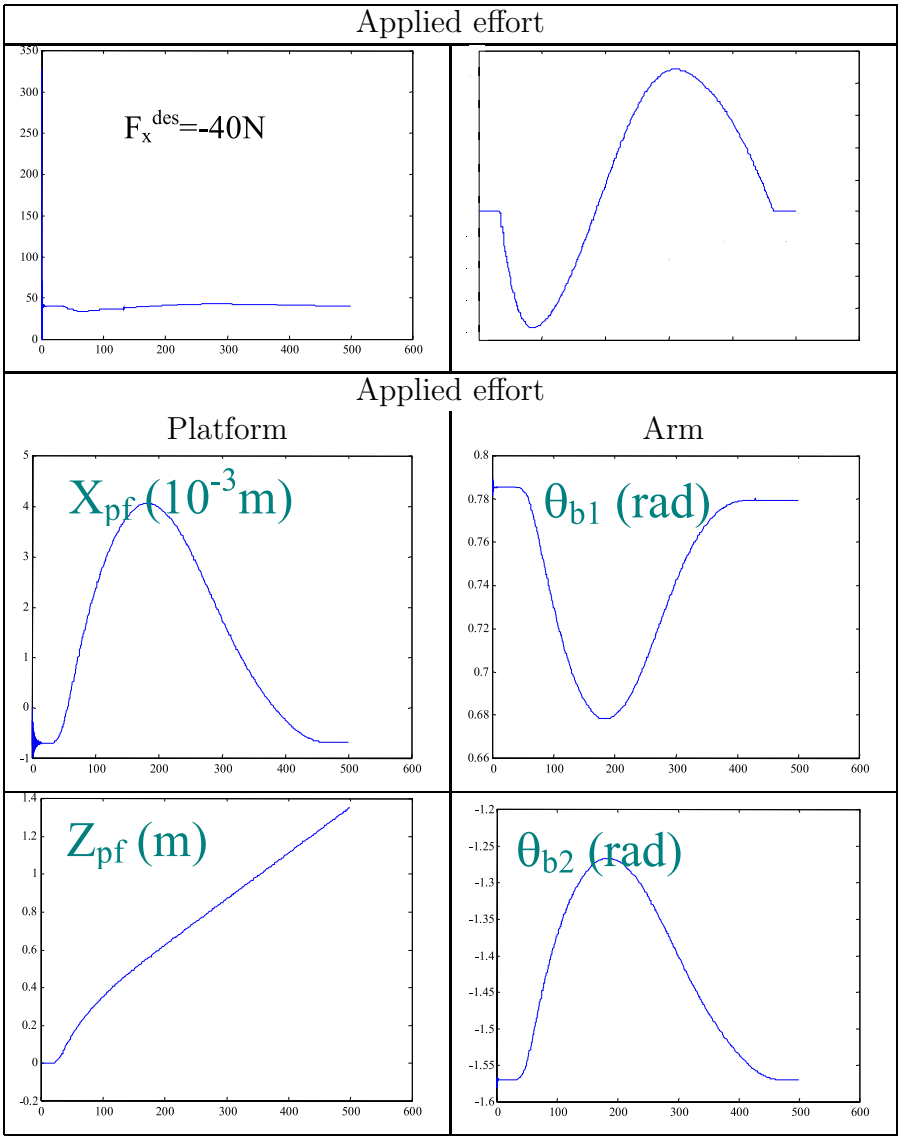


Table 7: force control on a trajectory, results

this control method, only measuring the torques present on the robot links. When the arm is moving in free space, it induces a reaction that can be modeled in two dimensions with a linear force and a reaction torque present on the link between the arm and the platform (figure 20).

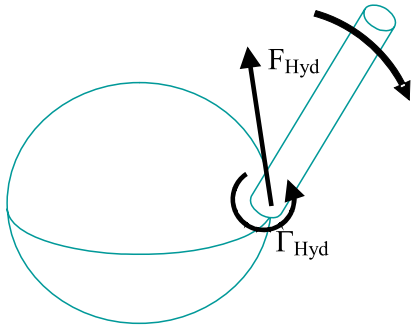


Figure 20: reaction effort

A complete force sensor can bring all the components of the arm action. If we reduce the interaction measurement to the torque $\Gamma_{Hyd}$, we have to consider a method to counteract the linear reaction of the arm. Inspired by the N. Kato's work on fish robot with apparatus pectoral fin motion [9], we can imagine to compensate the effects of the arm with a mechanical structure which acts like a fin, or a paddle (figure 21). It's installed on the platform and controlled by the measured torque (on the link between the arm and the vehicle) to produce on the platform the opposite arm action. This virtual fin has to be conformed to the geometrical hydrodynamic characteristics of the arm, to produce an action on the platform which compensate the arm effects.

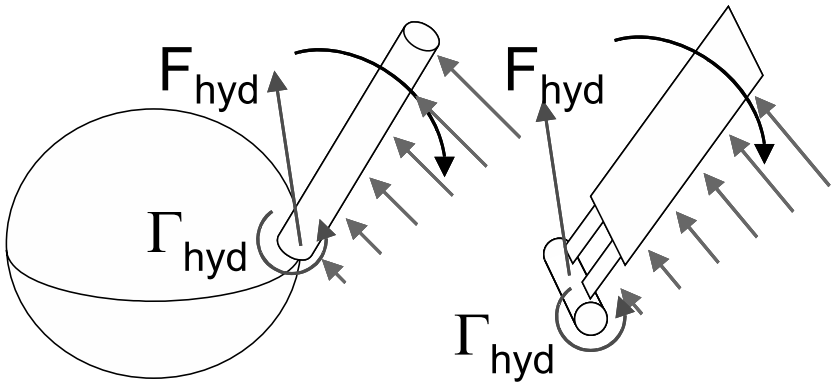


Figure 21: the virtual fin

We have chosen to symbolize the virtual fin as a rectangle. But a specific

study about the fin geometry has to be made to find out the optimal shape which guaranties the equivalence between the arm and the virtual fin actions. The virtual fin is linked on the platform on a specific point which govern the compensation strategy, and a dualism torque/linear compensation exists (figure 22).

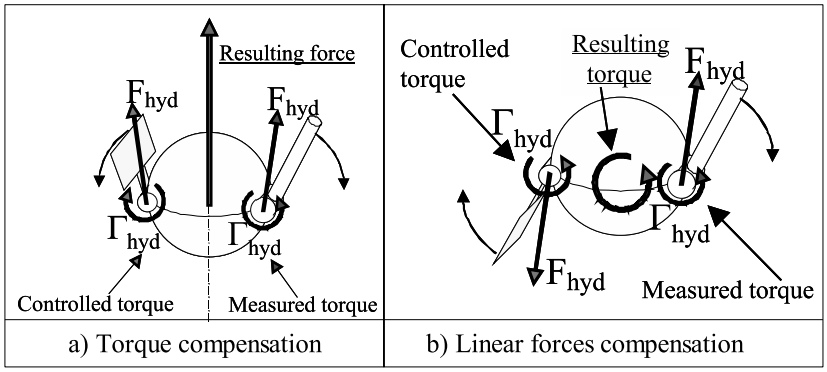


Figure 22: dualism torque/linear compensation

We have chosen to use only the measured reaction torque, and an implicit linear compensation is necessary, but involves a resulting torque on the platform (figure 22b). Therefore, this resulting torque is known and can be easily compensated with a paddle wheel structure mounted on the buoyancy center of the platform (figure 23).

The principal advantage of this compensation method is that it can be used outside the robot control loop, and counterbalance the arm action without any hydrodynamic parameters identification necessity.

# 9 Conclusion

This paper aimed at proposing and analyzing a control method to compensate for the disturbances produced by a manipulator motion on the underwater vehicle carrying it. Simulation results performed with a realistic simulator have proved the efficiency of our approach. The proposed method can be used during a force control task of the arm, which have to act on the environment, only modifying the desired effort vector, according to the task. A redundancy appears on the system, which can be ruled considering the different dynamics of the system component (arm and vehicle). Considering the difficulties to install a force sensor on a submarine system ( between the arm and the vehicle), we are currently investigating the performance we

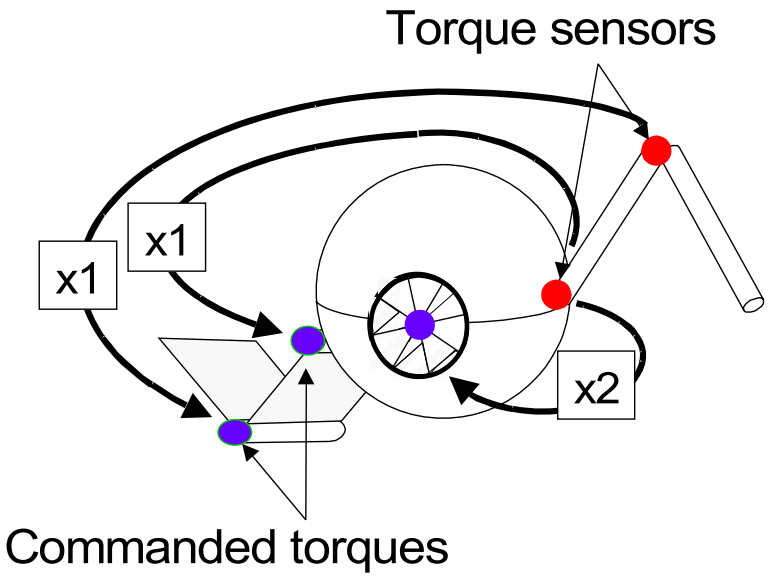


Figure 23: Implicit compensation structure

could obtain if only joint torque sensors can be used. This implies to install on the platform a mechanical structure which compensate the linear reaction of the arm at its base. This implicit compensation can be realised outside the control loop of the robot, only reproducing the measured torques on the compensation structure. This method avoids the on-line estimation of hydrodynamic coefficient.

# References

[1] DELEBARRE X. : "*Commande position force de deux bras manipulateurs pour l'exploration planetaire*", Thèse soutenue le 4 Juin 1992 au LIRMM, Montpellier, France.

[2] OLGUIN DIAZ E. : "*Modelisation et Commande d'un Systeme VÚhicule/Manipulateur Sous-marin*", Thèse soutenue le 11 Janvier 1999 Ó l'INPG, Grenoble, France.

[3] DUBOWSKY S., VANCE E.E. : "*Planning Mobile Manipulator Motions Considering Vehicle Dynamic Stability Contraints*", Proc. of the IEEE Int. Conf. on Robotics and Automation, Scottdale, Arizona, 1989, pp.1271-1276.

[4] DUNNIGAN M.W., RUSSEL G. T. : "*Evaluation and Reduction of the Dynamic Coupling Between a Manipulator and an Underwater Vehicle*", IEEE Journal of Ocean Engineering, , Vol 23, Num. 3, July 98, pp 260-274.

[5] FALTINSEN O.M. : "*Sea loads on ships and offshore structures*", Cambridge University Press, 1st. ed., 1990.

[6] FRAISSE P. : "*Contribution à la commande robuste position/force des robots manipulateurs à architecture complexe : application à un robot à deux bras* ", These soutenue le 17 Fevrier 1994 au LIRMM, Montpellier, France.

[7] FOSSEN T.I. : "*Guidance and Control of Ocean Vehicles*", John Wiley and Sons, New York, 1st. ed., 1994.

[8] GOLDSTEIN R.J. : "*Fluid Mechanics Measurements*", Hemisphere Publishing Corporation, $1^{st}$. ed., 1976.

[9] KATO N., LANE D.M. : "*Coordinated Control of Multiple Manipulators in Underwater Robots*", Proc. of IEEE Int. Conf. on Robotics and Automation, Minneapolis, Minnesota, 1996, pp. 2505-2510.

[10] KIENER J. : "*Coupled Vehicle and Manipulator Modeling and Control : Scope of the work*", UNION Project, ESPRIT BRA #8972 - D5.6, 1996.

[11] McLAIN T.W., ROCK S.M., LEE M.J. : "*Experiments in the Coordination Control of an Underwater Arm/Vehicle System*", IEEE Journal of Autonomous Robots, Vol. 3(2 and 3), 1996.

[12] MA B., HUO W. : "*Adaptive Control of Space Robot System with an Attitude Controlled Base* ", Proc. of the IEEE Int. Conf. on Robotics and Automation, Nagoya, Japon, 1995, pp. 1265-1270.

[13] MAHESH H. : YUH J., LAKSHMI R. : "*A Coordinated Control of an Underwater and Robotic Manipulators*", Journal of Robotic System, Vol. 8,n 3, June 1991, pp. 339 - 370.

[14] NEWMAN J.N. : "*Marine hydrodynamics*", Cambridge, MIT Press, $1^{st}$ ed., 1977.

[15] ODA M. : "*Coordinated Control of Spacecraft Attitude and its Manipulator*", Proc. of IEEE Int. Conf. on Robotics and Automation, Minneapolis, Minnesota, April, 1996, pp. 732 - 738.

[16] PERDEREAU V. : "*Contribution à la commande hybride position-force*", Thèse soutenue le 18 fÚvrier 1991 Ó l'UniversitÚ Pierre et Marie CURIE, Paris, France.

[17] PIN F.G., CULIOLI J.C. : "*Multi-Criteria Position and Configuration Optimization for Redundant Platform/Manipulator Systems*", Proc. of the IEEE Int. Workshop on intelligent Robots and Systems, Tsuchiura, Japon, 1990, pp. 103-107.

[18] SERAJI H. : "*An On-line Approach to Coordinated Mobility and Manipulation*", Proc. of the 1993 IEEE Int. Conf. of Robotics and Automation, Atlanta, Georgie, 1993.

[19] S.N.A.M.E. : "*Nomenclature for Treating the Motion of a Submerged Body Through a Fluid*", Technical and Research Bulletin n I-5 The society of Naval Architects and Marine Engineers, Oct 1964 (SNAME) New York.

[20] YAMAMOTO Y., YUN X. : "*Coordinating Locomotion and Manipulation of a Mobile Manipulator*", Proc. of the $31^{st}$ Conf. on decision and Control, Tucson, Arizona, 1992, pp. 2643-2648.

[21] YAMAMOTO Y., YUN X. : "*Control of Mobile Manipulation Following a Moving Surface*", Proc. of the 1993 IEEE Int. Conf. of Robotics and Automation, Atlanta, Georgie, 1993.

[22] YUH J. : "*Control of Underwater Robotic Vehicles*", Int. IEEE Journ. on Transaction on Systems, Man, and Cybernetics, Vol 20, N 6, 1990.

[23] YUH J. : "*Control Of Underwater Robotic Vehicles*", Proc. of IEEE/RSJ Int. Conf. on Intelligent Robots and Systems, Yokohama, Japan, July 26 - 30, 1993.